

Significance of interface anisotropy in laser induced magnetization precession in ferromagnetic metal films

D. Wang*

*Department of Physics, National University of Defense Technology,
Changsha 410073, Hunan, P. R. China*

A. J. Schellekens[†] and B. Koopmans

*Department of Applied Physics, Center for NanoMaterials (cNM),
Eindhoven University of Technology, P.O. Box 513,
5600 MB, Eindhoven, The Netherlands*

(Dated: March 9, 2019)

Abstract

Laser induced ultrafast demagnetization in ferromagnetic metals was discovered almost 20 years ago, but currently there is still lack of consensus on the microscopic mechanism responsible for the corresponding transfer of angular momentum and energy between electron, lattice and spin sub-systems. A distinct, but intrinsically correlated phenomenon occurring on a longer timescale is the magnetization precession after the ultrafast demagnetization process, if a magnetic field is applied to tilt the magnetization vector away from its easy direction, which can be attributed to the change of anisotropy after laser heating. In an in-plane magnetized Pt/Co/Pt thin film with perpendicular interface anisotropy, we found excellent agreement between theoretical prediction with plausible parameters and experimental data measured using time resolved magneto-optical Kerr effect. This agreement confirms that the time evolution of the anisotropy field, which is driven by the interaction between electrons and phonons, determines the magnetization precession completely. A detailed analysis shows that, even though the whole sample is magnetized in-plane, the dynamic interface anisotropy field dictates the initial phase of the magnetization precession, highlighting the significance of the interface anisotropy field in laser induced magnetization precession.

PACS numbers: 75.78.-n, 75.78.Jp

Since the first experimental demonstration of ultrafast demagnetization in ferromagnetic Ni in 1996¹, the interplay between coherent light and magnetic order has attracted much attention in the magnetism community². The physics involved in the laser induced ultrafast demagnetization is so complicated that, after almost 20 years of its discovery, the microscopic mechanism responsible for the transfer of angular momentum between electron, spin and lattice subsystems, upon irradiation by laser pulses, remains elusive. Possible candidates include direct angular momentum transfer from photons to electrons³, electron-phonon scattering^{4,5}, electron-magnon scattering⁶, electron-electron scattering⁷, and coherent interaction between electrons and photons⁸. In contrast to these local dissipation channels, superdiffusive transport due to the different lifetime for spin-up and spin-down electrons was proposed to account for the demagnetization observed in the first several hundred femtoseconds after laser irradiation^{9,10}. For a complete description of the laser induced ultrafast demagnetization in ferromagnets, all of those processes should be included in a Boltzmann-like approach¹¹.

A related phenomenon occurring on a longer timescale is the laser induced magnetization precession in ferromagnetic metals^{12,13}. Depending on the anisotropy of the studied material, the precession period can vary drastically. But the typical timescale is ~ 100 ps. The magnetization precession observed can be understood on the basis of the change of the anisotropy, which is a sensitive function of temperature. Intuitively, the two processes, i.e. the ultrafast demagnetization occurring on the timescale of 100 fs and the magnetization precession with periods of about 100 ps, are connected to each other. Actually, with a three temperature model, the magnetization precession was explained as a consequence of the dynamic temperature profile, which is just the driving force for the ultrafast demagnetization¹⁴. It was found that the qualitative behavior for films with in-plane anisotropy and out-of-plane anisotropy is different, but no quantitative conclusion was given. A similar attempt using the Landau-Lifshitz-Bloch equation¹⁵ was made later¹⁶. The aim of this article is to quantify the significance of different types of anisotropy, based on a model description of the magnetization precession.

In our model description, the ultrafast demagnetization is described by the microscopic three temperature model (M3TM)⁵, and the transverse relaxation of magnetization is given by the phenomenological LLG equation^{17,18}. Hence, if only heat dissipation along the film normal (z direction) is considered, the magnetization dynamics is given by three coupled

differential equations⁵,

$$\begin{aligned}
C_e \frac{dT_e}{dt} &= \nabla_z (\kappa \nabla_z T_e) + g_{ep}(T_p - T_e) + P(t), \\
C_p \frac{dT_p}{dt} &= g_{ep}(T_e - T_p), \\
\frac{d\mathbf{m}}{dt} &= RT_p \left(1 - m \coth \left(\frac{mT_C}{T_e} \right) \right) \mathbf{m} \\
&\quad - \gamma \left(\mathbf{m} \times \mathbf{B} + \alpha \frac{\mathbf{m}}{m} \times (\mathbf{m} \times \mathbf{B}) \right). \tag{1}
\end{aligned}$$

T_e and T_p are the electron and phonon temperatures, $C_e = \gamma T_e$ and C_p are the corresponding heat capacities. For a free electron gas, $\gamma = \pi^2 D_F k_B^2 / 3V_{at}$ with D_F the electronic density of states at the Fermi energy, k_B the Boltzmann constant and V_{at} the atomic volume. ∇_z denotes the z component of the gradient operator. Source term $P(t)$ is related to the heating effect caused by laser pulses, which are assumed to couple directly to the electron subsystem. The three subsystems are assumed to be at equilibrium, energy and angular momentum only flow between them. $\mathbf{m} = \mathbf{M}/M_0$, whose magnitude is m , is the magnetization vector normalized to the zero temperature saturation magnetization M_0 , γ is the gyromagnetic ratio, and α is the phenomenological Gilbert damping constant. \mathbf{B} is the total effective magnetic field, including the external, anisotropy and demagnetization field contributions. T_C is the Curie temperature, κ is the electronic thermal conductivity constant of the ferromagnetic metal, and g_{ep} is the phenomenological electron-phonon coupling constant. g_{ep} is assumed to be a constant, although it is actually a temperature dependent quantity¹⁹. Microscopically, g_{ep} can be related to microscopic parameters as

$$g_{ep} = \frac{3\pi D_F^2 D_p E_D k_B}{2 V_{at} \hbar} \lambda_{ep}^2, \tag{2}$$

where \hbar is the reduced Planck's constant, D_p is the number of atoms per atomic volume, E_D is the Debye energy, and λ_{ep} is the microscopic electron-phonon coupling constant. Constant R determines the demagnetization rate, and is related to the spin-flip probability α_{sf} during electron-phonon collisions, mediated by the spin-orbit coupling, through

$$R = \frac{8\alpha_{sf} g_{ep} k_B T_C}{E_D^2 \mu_{at}} \tag{3}$$

with μ_{at} the number density of Bohr magnetons for the ferromagnet. Compared to the M3TM⁵, the main modification made here is the addition of the transverse relaxation term to the equation of motion for the magnetization vector. In spirit, the separation of the

magnetization dynamics into longitudinal and transverse relaxations used here is similarly employed in the LLB equation¹⁵ and the self-consistent Bloch equation²⁰. The only difference lies in the longitudinal relaxation term, which is given here by the M3TM⁵.

To quantify the influence of anisotropy field using Eq. (1), the magnetization dynamics of a thin Co film was studied. The sample investigated was a Pt (4 nm)/Co (4 nm)/Pt (2 nm) film made by DC magnetron sputtering onto a Boron doped Silicon wafer with 100 nm thermally oxidized SiO₂. The base pressure of the sputtering chamber was 5.0×10^{-8} mbar. The sputtering pressure for Pt was 3.0×10^{-3} mbar, while it was 1.0×10^{-2} mbar for Co. The sputtering rate is 1.16 Å/s for Pt and 0.29 Å/s for Co. Time-resolved magneto optical Kerr effect (TRMOKE) measurements were performed using a pulsed Ti:Sapphire laser with central wavelength 780 nm, pulse width 70 fs and repetition rate 80 MHz. Both pump and probe beams were focused onto the sample at almost normal incidence, hence the measured TRMOKE signal is most sensitive to the out-of-plane (z) component of the magnetization. The laser pump pulses induced, delay time (Δt) dependent Kerr rotation was recorded using a double modulation technique²¹. In the TRMOKE measurements, the external magnetic field was applied almost normal to the film plane (xy plane), in order to tilt the magnetization out of the film plane.

It is well known that, at Pt/Co interfaces, the interface anisotropy is perpendicular to the film plane, due to the $3d$ - $5d$ hybridization there^{22,23}. Assuming negligible bulk anisotropy, the total anisotropy is a sum of the interface anisotropy and the demagnetization anisotropy,

$$E_A = - \left(K_s \frac{m^3(T_p)}{m^2} - K_d \right) m_z^2, \quad (4)$$

where K_s and $K_d = \mu_0 M_0^2 / 2$ are the temperature independent, interface and demagnetization anisotropy constants. The temperature dependence of the interface anisotropy is taken into account explicitly in Eq. (4) by the term cubic^{24,25} in m . Note we have postulated that the interface anisotropy is sensitive to the lattice temperature T_p , as it is primarily determined by the crystal field¹⁴. Due to the interface character of K_s , there is a critical Co thickness where transition from out-of-plane magnetized configuration to in-plane magnetized configuration occurs. This thickness is around 1 nm for our sputtered samples²⁶. Hence for the 4 nm Co film considered here, the demagnetization anisotropy dominates the interface anisotropy, and the film plane is the magnetic easy plane. Corresponding to Eq.

(4), the anisotropy field is given by

$$\mathbf{B}_K = \left(B_s \frac{m^3(T_p)}{m^2} - B_d \right) m_z \hat{\mathbf{e}}_z = (B_A + B_D) \hat{\mathbf{e}}_z, \quad (5)$$

where $B_s = 2K_s/M_0$, $B_d = \mu_0 M_0$ and $\hat{\mathbf{e}}_z$ is a unit vector perpendicular to the film plane.

In order to numerically study the laser induced magnetization dynamics, the Co film was divided into four layers. The top layer and the bottom layer are affected by both the interface anisotropy field and the demagnetization field, while the middle layers are only influenced by the demagnetization field, which is obtainable from Eq. (5) by setting $B_s = 0$. The exchange coupling between adjacent layers, layer i and layer j , is modelled by the standard expression

$$E_X = \frac{A}{d^2} \mathbf{m}_i \cdot \mathbf{m}_j, \quad (6)$$

with $d = 1$ nm being the separation between adjacent layers and $A = 28$ pJ/m the exchange stiffness constant for thin film Co^{27,28}. The laser pulse $P(t)$ was modeled by a gaussian function with group velocity dispersion²⁹. The optical penetration depth at 780 nm of Co is 13.5 nm³⁰. Except for the magnitude of the laser pulse, all other optical parameters used in the simulation were extracted from numerically fitting the short timescale (<1 ps) demagnetization data, using a phenomenological model given in Ref. 31. Bulk magnetic parameters³², $T_C = 1388$ K, $V_{at} = 11.1 \text{ \AA}^3$, $M_0 = 1.72 \mu_B/V_{at}$, $\mu_{at} = 1.72/V_{at}$, were adapted in the fit to experimental data using Eq. (1). The Debye energy $E_D = 38.4$ meV of Co³³ was also fixed in the fit to data. The thermal conductivity of a 15 nm thick Co film $\kappa = 40$ W/m K³⁴ was used to simulate the heat flow between individual magnetic layers. The heat exchange between the Co film and the substrate is treated simply by a phenomenological thermal conductivity κ_{sub} , which is varied to fit the data. The substrate temperature is set to the ambient temperature, $T_{am} = 300$ K.

Experimental TRMOKE traces and best fits are shown in Fig. 1, after subtracting the state filling effect contribution³⁵ at $\Delta t = 0$ to the experimental data. In fitting to the experimental data, the measured magneto-optical signal, MO , is assumed to have contributions from all three components of the magnetization vector^{36,37}, $MO \propto m_z + \alpha_x m_x + \alpha_y m_y$, given that in our experimental setup, the probe light is not exactly normal to the film plane. Then the variation of the magneto optical signal, ΔMO , which is defined as the difference after and before the arrival of the laser pulse, is normalized to the maximal demagnetization, ΔMO_{max} , as shown in Fig. 1. The normalized data is then fitted by Eq. (1). Details of

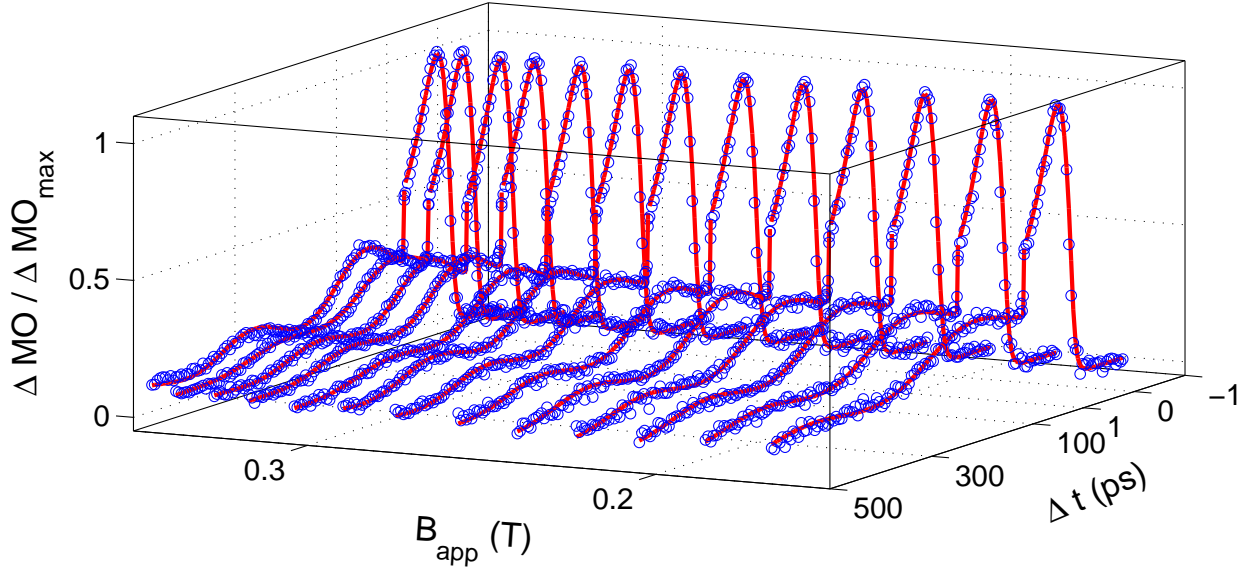


FIG. 1. Experimental magneto optical traces with various applied field (B_{app}) normalized to the maximal signal, ΔMO_{max} . Note the change of scale at delay time $\Delta t = 1$ ps. Blue circles are experimental data, and red lines are the corresponding fits. Distinctive features in magnetization dynamics induced by ultrashort laser pulses irradiating on ferromagnetic metals are discernible: ultrafast demagnetization occurring on the timescale of < 1 ps and magnetization precession on ~ 100 ps timescale.

the fitting procedure can be found in Ref. 5. It can be seen from Fig. 1 that the overall agreement between experiment and theory is satisfactory, considering the crudeness of our model. This shows that the main physics is captured by the simple Eq. (1). The relevant physical parameters obtained from the best fits are $\alpha_{sf} = 0.16 \pm 0.01$, $\alpha = 0.07 \pm 0.02$, $\gamma = 1.64 \pm 0.06$, $B_s = 1.50 \pm 0.01$ T, $\lambda_{ep} = 11.3 \pm 0.3$ meV. The errors given are the standard deviation of fitted values corresponding to different applied field B_{app} . The fitted γ corresponds to a Landé g-factor $g = 1.86 \pm 0.07$, which is very close to the free electron value. The interface anisotropy gives an out-of-plane to in-plane transition thickness ~ 1.7 nm at zero temperature. This value is slightly larger than the experimental value ~ 1 nm. Since we used the bulk T_C and μ_{at} in the fitting procedure, this difference is still acceptable. Finally, the Elliott-Yafet spin-flip probability α_{sf} and the electron-phonon coupling constant λ_{ep} are comparable to those obtained in Ref. 5.

To get a holistic understanding of the magnetization precession, the time evolution of the total anisotropy field B_K for the top Co layer is plotted in Fig. 2, together with its two

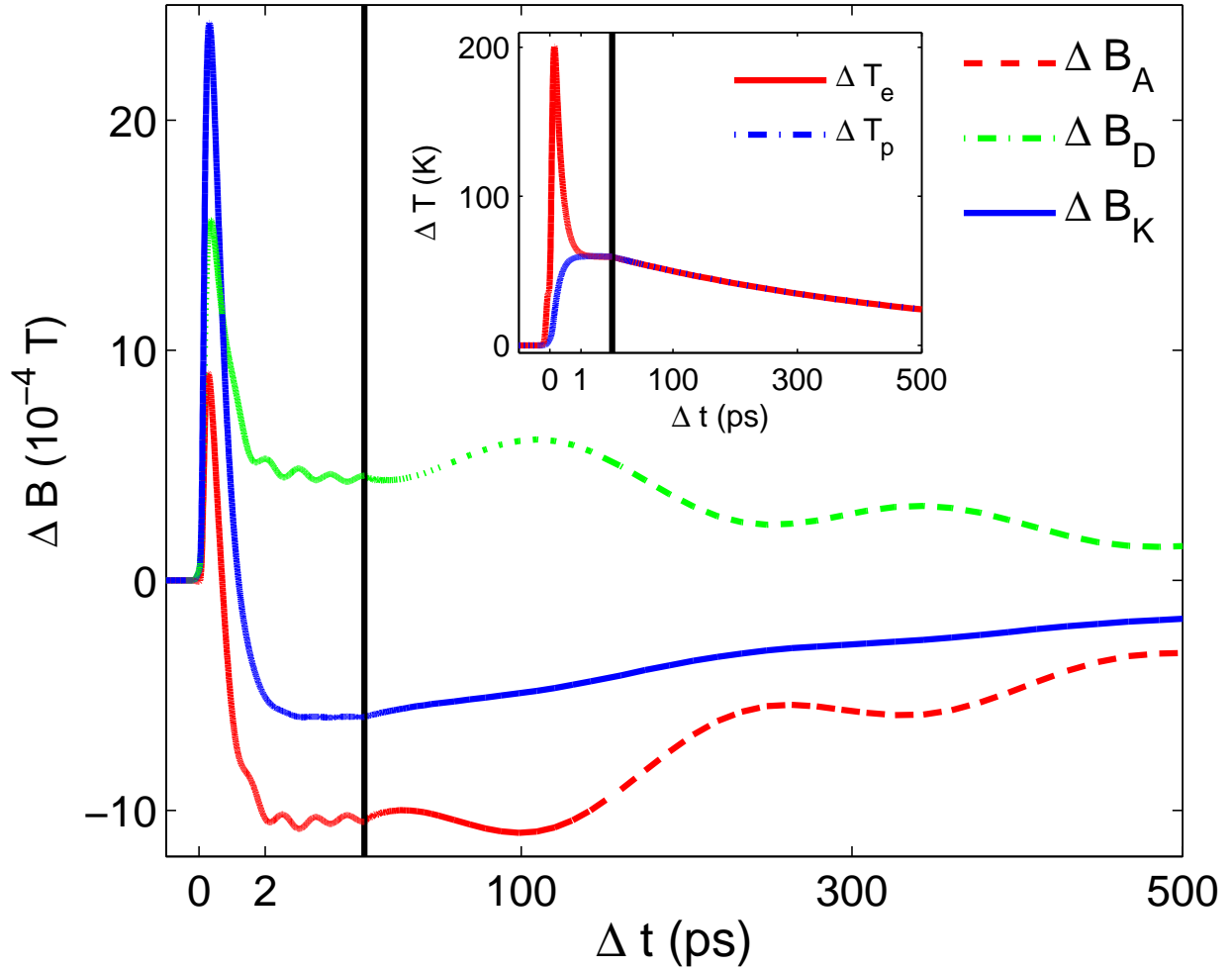


FIG. 2. Dynamic evolution of the anisotropy field (B_A , dashed line), the demagnetization field (B_D , dash-dotted line) and the total effective field (B_K , solid line) for the top Co layer with $B_{app} = 0.29$ T. The inset shows the change of the electron temperature and the lattice temperature with delay time Δt . Note the change of scale at $\Delta t = 5$ ps (2 ps in the inset) delineated by the vertical solid line. The small amplitude ringing structure visible in ΔB_D and ΔB_A is caused by the interlayer exchange coupling. It will be attenuated to zero in about 20 ps.

competing components, the interface anisotropy field and the demagnetization field. The main characteristics of Fig. 2 is that, while the short timescale variation of B_D and B_A is both positive, ΔB_D and ΔB_A are of opposite signs at large timescale. This competition results in a negative anisotropy change, as shown in Fig. 2. The positive change of the demagnetization field is easily understandable. From Eq. (5), ΔB_D is essentially the change of the z component of the magnetization vector. With the elevation of temperature (c.f.

inset of Fig. 2), the magnitude of the magnetization vector is always reduced, therefore the change of the demagnetization field is always positive. The sign change of ΔB_A is intriguing. It is a natural result of the dynamic evolution of T_e and T_p , which is itself the driving force for the ultrafast demagnetization observed at short timescale ($\Delta t < 1$ ps in Fig. 1). As can be seen in the inset of Fig. 2, before the equilibrium is reached, the electron temperature T_e is higher than the phonon temperature T_p . From Eq. (5), a higher T_e , whose direct consequence is a smaller m ($< m(T_p)$), will give a positive change of B_A , compared with the value before the arrival of the laser pulses. Once an equilibrium is established between T_e and T_p (Actually, in the inset of Fig. 2, there is a small amplitude overshooting of the phonon temperature, which is solely resulted from the fact that only the heat dissipation due to electron heat conduction is considered in Eq. (1)), their common value is still higher than the ambient temperature, $T \approx T_e \approx T_p > T_{am}$. This results in $B_A \propto mm_z(T)$, which is smaller than its corresponding value at ambient temperature, assuming the polar angle of \mathbf{m} (hence m_z) is not increased in the whole process (Fig. 2, ΔB_D curve). The resulted change of anisotropy is thus negative. The above analysis qualitatively explains the change of sign for ΔB_K , and hence the initial phase of the magnetization precession. Without the sign change in ΔB_K , the magnetization precession will follow the ΔB_D curve. In addition, more insight into the magnetization precession observed can be gained: the driving force behind the magnetization precession is the dynamic evolution of the anisotropy field, which is directly derived from the equilibration process of the electron and phonon subsystems initiated by irradiation of ultrashort laser pulses. This completes the whole picture of laser induced magnetization precession in ferromagnetic metal films.

To summarize, the laser pumped magnetization precession in Pt/Co/Pt thin film system with perpendicular interface anisotropy is investigated by time resolved magneto optical Kerr effect. Based on a microscopic three temperature model, a model description of the magnetization precession is proposed. It is found that the experimental data can be excellently fitted by the theoretical model. This agreement between theory and experiment provides insight into the different roles played by the demagnetization field and the interface anisotropy field in laser induced magnetization precession. Importantly, the initial phase of the precession is determined by the dynamic interface anisotropy field completely. Given the possible utilization of laser induced anisotropy change in controlling magnetization dynamics, especially in search of ultrafast switching of magnetization using laser pulses,

the proposed model description could serve as a starting point to explore more interesting physics in other systems, such as exchange-coupled artificial superlattices.

ACKNOWLEDGMENTS

This work was supported by the Foundation for Fundamental Research on Matter (FOM), which is part of the Netherlands Organization for Scientific Research (NWO).

* daowei_wang@hotmail.com

† a.j.schellekens@tue.nl

- ¹ E. Beaurepaire, J. C. Merle, A. Daunois, and J.-Y. Bigot, *Phys. Rev. Lett.* **76**, 4250 (1996).
- ² A. Kirilyuk, A. V. Kimel, and Th. Rasing, *Rev. Mod. Phys.* **82**, 2731 (2010).
- ³ G. P. Zhang and W. Hübner, *Phys. Rev. Lett.* **85**, 3025 (2000).
- ⁴ B. Koopmans, J. J. M. Ruigrok, F. Dalla Longa, and W. J. M. de Jonge, *Phys. Rev. Lett.* **95**, 267207 (2005).
- ⁵ B. Koopmans, G. Malinowski, F. Dalla Longa, D. Steiauf, M. Fähnle, T. Roth, M. Cinchetti, and M. Aeschlimann, *Nat. Mater.* **9**, 259 (2010).
- ⁶ E. Carpene, E. Mancini, C. Dallera, M. Brenna, E. Puppini, and S. De Silvestri, *Phys. Rev. B* **78**, 174422 (2008).
- ⁷ M. Krauss, T. Roth, S. Alebrand, D. Steil, M. Cinchetti, M. Aeschlimann, and H. C. Schneider, *Phys. Rev. B* **80**, 180407 (2009).
- ⁸ J.-Y. Bigot, M. Vomir, and E. Beaurepaire, *Nat. Phys.* **5**, 461 (2009).
- ⁹ M. Battiato, K. Carva, and P. M. Oppeneer, *Phys. Rev. Lett.* **105**, 027203 (2010).
- ¹⁰ M. Battiato, K. Carva, and P. M. Oppeneer, *Phys. Rev. B* **86**, 024404 (2012).
- ¹¹ B. Y. Mueller, T. Roth, M. Cinchetti, M. Aeschlimann, and B. Rethfeld, *N. J. Phys.* **13**, 123010 (2011).
- ¹² M. van Kampen, C. Jozsa, J. T. Kohlhepp, P. LeClair, L. Lagae, W. J. M. de Jonge, and B. Koopmans, *Phys. Rev. Lett.* **88**, 227201 (2002).
- ¹³ M. van Kampen, B. Koopmans, J. T. Kohlhepp, and W. J. M. de Jonge, *J. Magn. Magn. Mater.* **240**, 291 (2002).

- ¹⁴ J.-Y. Bigot, M. Vomir, L. H. F. Andrade, and E. Beaurepaire, *Chem. Phys.* **318**, 137 (2005).
- ¹⁵ N. Kazantseva, D. Hinzke, U. Nowak, R. W. Chantrell, U. Atxitia, and O. Chubykalo-Fesenko, *Phys. Rev. B* **77**, 184428 (2008).
- ¹⁶ U. Atxitia, O. Chubykalo-Fesenko, N. Kazantseva, D. Hinzke, U. Nowak, and R. W. Chantrell, *Appl. Phys. Lett.* **91**, 232507 (2007).
- ¹⁷ L. D. Landau, E. M. Lifshitz, and L. P. Pitaevski, *Statistical Physics*, Part 2, 3rd ed. (Pergamon, Oxford), 1980.
- ¹⁸ T. L. Gilbert, *IEEE Trans. Mag.* **40**, 3443 (2004).
- ¹⁹ Z. Lin, L. V. Zhigilei, and V. Celli, *Phys. Rev. B* **77**, 075133 (2008).
- ²⁰ L. Xu and S. Zhang, *Physica E* **45**, 72 (2012).
- ²¹ B. Koopmans, M. van Kampen, J. T. Kohlhepp, and W. J. M. de Jonge, *J. Appl. Phys.* **87**, 5070 (2000).
- ²² P. Bruno, *Phys. Rev. B* **39**, 865 (1989).
- ²³ J. Stöhr, *J. Magn. Magn. Mater.* **200**, 470 (1999).
- ²⁴ E. Callen and H. B. Callen, *Phys. Rev.* **139**, A455 (1965).
- ²⁵ K. Kisielewski, A. Kirilyuk, A. Stupakiewicz, A. Maziewski, A. Kimel, Th. Rasing, L. T. Baczewski, and A. Wawro, *Phys. Rev. B* **85**, 184429 (2012).
- ²⁶ R. Lavrijsen, *Another spin in the wall: Domain wall dynamics in perpendicularly magnetized devices*, p. 43, PhD thesis, Eindhoven University of Technology, The Netherlands, 2011; <http://alexandria.tue.nl/extra2/693486.pdf>.
- ²⁷ X. Liu, M. M. Steiner, G. A. Prinz, R. F. C. Farrow, and G. Harp, *Phys. Rev. B* **53**, 12166 (1996).
- ²⁸ M. Grimsditch, E. E. Fullerton, and R. L. Stamps, *Phys. Rev. B* **56**, 2617 (1997).
- ²⁹ J.-C. Diels and W. Rudolph, *Ultrashort laser pulse phenomena*, 2nd ed. (Academic Press, San Diego), 2006.
- ³⁰ G. S. Krinchik and V. A. Artemjev, *J. Appl. Phys.* **39**, 1276 (1968).
- ³¹ G. Malinowski, F. Dalla Longa, J. H. H. Rietjens, P. V. Paluskar, R. Huijink, H. J. M. Swagten, and B. Koopmans, *Nat. Phys.* **4**, 855 (2008).
- ³² J. Stöhr, and H. C. Siegmann, *Magnetism: From Fundamentals to Nanoscale Dynamics*, (Springer, Berlin), 2006.
- ³³ C. Kittel, *Introduction to solid state physics*, 8th ed. (John Wiley & Sons, New Jersey), 2005.

- ³⁴ F. K. Dejene, J. Flipse, and B. J. van Wees, *Phys. Rev. B* **86**, 024436 (2012).
- ³⁵ B. Koopmans, M. van Kampen, J. T. Kohlhepp, and W. J. M. de Jonge, *Phys. Rev. Lett.* **85**, 844 (2000).
- ³⁶ Z. J. Yang and M. R. Scheinfein. *J. Appl. Phys.* **74**, 6810 (1993).
- ³⁷ Z. Q. Qiu and S. D. Bader, *Rev. Sci. Instrum.* **71**, 1243 (2000).